



Valence, hybridization of electronic states and magnetic properties of $\text{La}_{0.7}\text{Ca}_{0.3}\text{Mn}_{1-x}\text{Sc}_x\text{O}_3$ ($x = 0.0$; 0.03 , and 0.05) manganites

A.N. Ulyanov^{a,*}, Dong-Seok Yang^b, Hyun-Joon Shin^c, Ki-jeong Kim^c, A.V. Vasiliev^a, S.V. Savilov^a



^a Department of Chemistry, Lomonosov Moscow State University, Moscow, 119991, Russia

^b Department of Physics Education, Chungbuk National University, Cheongju, 28644, Republic of Korea

^c Pohang Accelerator Laboratory, POSTECH, Pohang, 37673, Republic of Korea

ARTICLE INFO

Article history:

Received 15 February 2019

Received in revised form

25 April 2019

Accepted 26 April 2019

Available online 28 April 2019

Keywords:

B-site doped manganites

Electron structure

Curie temperature

XAFS

ABSTRACT

X-ray absorption spectroscopy at Mn *K*- and *L*-edges, and at O *K*-edge, combined with the x-ray diffraction and magnetization measurements are performed to study the electron structure of $\text{La}_{0.7}\text{Ca}_{0.3}\text{Mn}_{1-x}\text{Sc}_x\text{O}_3$ ($x = 0.0$; 0.03 , and 0.05) perovskites. Substitution of manganese by scandium decreases Curie temperature, T_c , and increases lattice parameters because of the different electron configuration and radii of trivalent manganese and scandium ions. The T_c decrease is explained by the change of level of hybridization of O $2p$ and Mn $3d$ states. This is manifested by the parallel shift of O *K*-edge, change of intensity of $2p_{3/2}$ and $2p_{1/2}$ spectrum lines and T_c with x increase. Fourier transform of the EXAFS spectra shows a change of local crystal structure caused by the larger Sc^{3+} than the Mn^{3+} ions.

© 2019 Published by Elsevier B.V.

1. Introduction

Study of rare-earth manganese oxides (manganites) attracts considerable interest because of colossal magnetoresistivity (CMR) effect observed [1]. Parent LaMnO_3 perovskites are antiferromagnetic insulator with trivalent manganese. Partial substitution of lanthanide by divalent alkali-earth elements, D , leads to mixed $\text{Mn}^{3+}/\text{Mn}^{4+}$ valence causing the ferromagnetic ordering and conductivity in doped $\text{La}_{1-z}\text{D}_z\text{MnO}_3$ perovskites. Properties of the oxides are described at the frame of extended Zener double exchange (DE) model [2]. According to the model the ferromagnetism and metallic character of conductivity originate from the transfer of itinerant e_g electrons inside the Mn^{4+} matrix. Properties of manganites depend on doping in the A – position [1,3,4] and oxygen deficiency [5,6] in perovskite ABO_3 cell, and vacancies and stress accommodations in the crystal lattice [7,8].

At present, high attention is also paid for the study of B – site substituted $(\text{La}_{1-z}\text{D}_z)\text{Mn}_{1-x}\text{M}_x\text{O}_3$ (M – (transitional) metal, Al, Si) manganites [9–13]. Substitution of the metal for manganese causes

a decrease of the density of the itinerant electrons. This leads to decrease of Curie temperature, magnetization and conductivity. Change of the above parameters depends on the electron configuration and ionic radius of the substituent. Phenomenological description of the manganites $\text{La}_{0.7}\text{Ca}_{0.3}\text{Mn}_{0.95}\text{M}_{0.05}\text{O}_3$ ($M = \text{Al}, \text{Ga}, \text{In}, \text{Sc}$, and Fe , as special case) was recently performed (M are trivalent ions with completed electron outer shells) [13]. Authors showed that the Curie temperature, T_c , is mostly depended on difference of electron configuration of M^{3+} and Mn^{3+} ions and partially on the change of local crystal structure because of difference of Mn^{3+} and M^{3+} ion radii. If the substitutions differ from those pointed above the explanation of properties becomes more complicated. Interesting, Ru substitution for Mn in $\text{Pr}_{0.75}\text{Na}_{0.25}\text{Mn}_{1-x}\text{Ru}_x\text{O}_3$ oxides weakened the Jahn-Teller effect, caused the suppression of the charge ordering and revived ferromagnetic interaction at $x = 0.01$. The substitution of Cu, Si and Fe for Mn in $\text{La}_{0.7}\text{Sr}_{0.25}\text{Na}_{0.05}\text{Mn}_{0.9}\text{Cu}_{0.1}\text{O}_3$ [14], $\text{La}_{0.6}\text{Gd}_{0.1}\text{Sr}_{0.3}\text{Mn}_{0.8}\text{Si}_{0.2}\text{O}_3$ [15], and $\text{La}_{0.7}\text{Ca}_{0.3}\text{Mn}_{1-x}\text{Fe}_x\text{O}_3$ [16] and $\text{La}_{0.67}\text{Sr}_{0.33}\text{Mn}_{1-x}\text{Fe}_x\text{O}_3$ [17] entailed the considerable value of magnetocaloric effect for above perovskites. The $\text{La}_{0.67-x}\text{Eu}_x\text{Ba}_{0.33}\text{Mn}_{0.85}\text{Fe}_{0.15}\text{O}_3$ ceramics can be used in electronic application because of high value of permittivity observed [18]. At the same time the change of properties of B -site substituted manganites in connection with the change of electron structure is not studied well enough. Moreover, there are some very

* Corresponding author.

E-mail addresses: a-ulyanov52@yandex.ru, a_n_ulyanov@yahoo.com (A.N. Ulyanov).

unclear results. For examples, observed XAFS Mn *K*-edge spectra for the $\text{La}_{0.7}\text{Ca}_{0.3}\text{Mn}_{1-x}\text{Sr}_x\text{O}_3$ ($x = 0.0$ and 0.1) oxides were completely identical, but the T_c (value of which is usually associated with the Mn *K*-edge position [3]), decreased drastically with x increase. To shed light for the change of electron structure of the noted perovskites the XANES measurements at Mn *K* – and *L* – edges, and O *K* – edge and EXAFS study at energy just beyond the Mn *K*-edge were performed. Taking into account the observed differences of change of properties of *B*-site doped oxides at low ($0.0 \leq x \leq 0.05$) and high ($x > 0.05$) doping [19,20], and to avoid an ambiguity in the description of properties caused by the level of substitution we present the study of low doped $\text{La}_{0.7}\text{Ca}_{0.3}\text{Mn}_{1-x}\text{Sc}_x\text{O}_3$ ($x = 0.0, 0.03$ and 0.05) samples.

2. Experimentals

The $\text{La}_{0.7}\text{Ca}_{0.3}\text{Mn}_{1-x}\text{Sc}_x\text{O}_3$ (LCMNSc) ($x = 0.0; 0.03$, and 0.05) oxides were prepared by nitrate technique using La_2O_3 oxide, CaCO_3 and ScCO_3 carbonates, and metallic manganese as starting materials. X-ray Cu *Ka* diffraction (XRD) analysis was performed with the diffractometer D/MAX-2500V/PC (Rigaku, Japan). The x-ray absorption fine structure (XAFS = XANES + EXAFS) measurements were performed at the Pohang Light Source, PLS (Republic of Korea) operating with an electron energy of 3.0 GeV and the maximum current of 400 mA. The measurements at Mn *K* edge were carried out at 8C Nano-XAFS beamline. The XANES measurements at O *K*-edge and Mn *L*-edges were performed at the total electron yield mode at PLS 10A2 beamline. The results for Mn *K*-edge, and O *K*-edge and Mn *L*-edges were calibrated using the reference spectra of manganese foil, and N_2 and O_2 molecules, respectively. Resolution of the beamline photon energy was about 2×10^{-4} . The magnetic susceptibility, χ , was measured in a field of 10 Oe and at a frequency of 27 Hz. Accuracy of the susceptibility measurement was ~5%, precision of the temperature measurement equaled to ± 2 K. Curie temperature was defined as the inflection point on the χ on T curves.

3. Results and discussions

The XRD patterns of the sintered manganites are presented in Fig. 1. According to analysis the $\text{La}_{0.7}\text{Ca}_{0.3}\text{Mn}_{1-x}\text{Sc}_x\text{O}_3$ perovskites are single phase and belong to orthorhombic *Pnma* singony. With x increase the lattice parameters of the oxides increase because the radius of the Sc^{3+} ($= 0.745$ Å) is larger than that of the Mn^{3+} ($= 0.645$ Å). Ionic radii are taken from the Shannon work [21]. XRD results are presented in Table 1 and are in line to those presented in

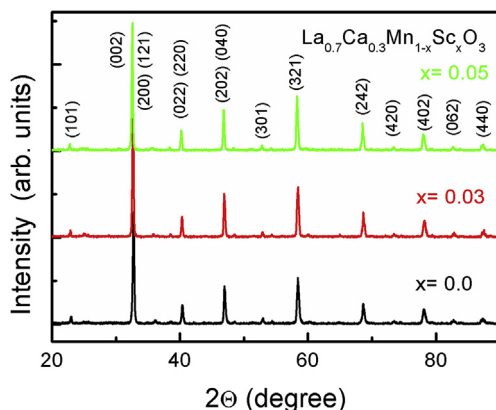


Fig. 1. XRD patterns for $\text{La}_{0.7}\text{Ca}_{0.3}\text{Mn}_{1-x}\text{Sc}_x\text{O}_3$ ($x = 0.0, 0.03$, and 0.05).

Table 1

Lattice parameters (a , b , c), cell volumes (V) and Curie temperature (T_c) for $\text{La}_{0.7}\text{Ca}_{0.3}\text{Mn}_{1-x}\text{Sc}_x\text{O}_3$ oxides.

x value	a (Å)	b (Å)	c (Å)	V (Å 3)	T_c (K)
0.0	5.4753	7.7281	5.4705	231.47	251.6
0.03	5.4826	7.7304	5.4782	232.18	158.0
0.05	5.4861	7.7323	5.4805	232.48	116.9

Error bars for the lattice parameters and cell volume equal to 0.0006 Å, and 0.01 Å 3 , respectively.

Ref. [22].

Fig. 2 presents the temperature dependence of AC susceptibility, $\chi(T)$, of the samples. Curie temperature decreases from 252 to 117 K which correspond to the change observed in Refs. [10,22]. The observed T_c decrease is mainly caused by the different electron configuration of Mn^{3+} and Sc^{3+} , and, partially, by the difference of the radii of the above ions (see [13], on this item).

XANES spectra of the LCMNSc manganites are presented in Fig. 3. The spectra show no essential change in shape and Mn *K*-edge position with x increasing. This indicates no change in average manganese valence, v_{Mn} . At the same time, the substitution of Sc^{3+} ions for the Mn^{3+} ions leads for decrease of the formal manganese valence from 3.3 (at $x = 0.0$) to 3.15 (at $x = 0.05$) causing the essential decrease of the T_c (see, also [10,22,23]). The result is similar to that observed at studying the self-doped $\text{La}_{1-x}\text{MnO}_{3+\delta}$ manganites where the formal manganese oxidation state and T_c changed with x increase but Mn *K*-edge position showed very weak change only [7,24]. Notable, in $\text{La}_{1-x}\text{Ca}_x\text{MnO}_3$ oxides the Mn *K*-edge position shifts for about 4.0 eV and T_c increases for about a few ten degrees at changing of Mn oxidation state from Mn^{3+} to Mn^{4+} with increase of z -value from zero to unit [3,4]. The results show a difference in manifestation of the change of formal/observed manganese valence and T_c at hole doping, and of the vacancy-doping and *B*-site substituting perovskites. Note, in $\text{Pr}_{0.67}\text{Sr}_{0.33}\text{MnO}_3$ [25] and $\text{La}_{1-x}\text{Ca}_x\text{MnO}_3$ [4] oxides a minor change of Mn *K* – pre-edge spectra with increase of temperature and z , respectively, were observed and attributed to the change of hybridization between Mn 3d and 4p neighboring orbitals. At the same time, the present study did not reveal any essential change at the Mn *K*-pre-edge spectra (see interval energy from 6540 to 6545 eV in Fig. 3).

Fourier transform of the EXAFS spectra are presented in the inset of Fig. 3. The Fourier transform shows a change of backscattering of electrons from the atoms located at coordination spheres associated with oxygen positions (OP) and lanthanum/calcium position (AP). The above positions correspond to first and second

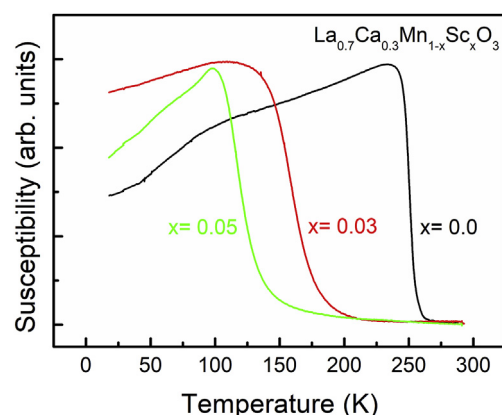


Fig. 2. Temperature dependencies of AC susceptibility for $\text{La}_{0.7}\text{Ca}_{0.3}\text{Mn}_{1-x}\text{Sc}_x\text{O}_3$ ($x = 0.0, 0.03$, and 0.05) perovskites.

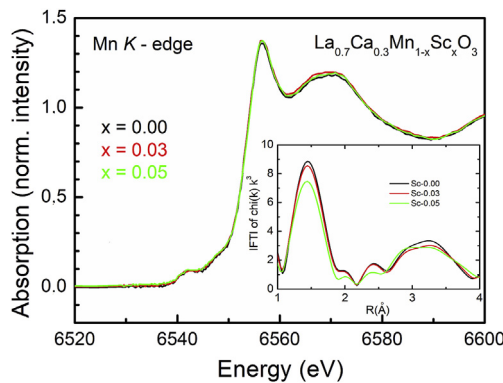


Fig. 3. Mn *K*-edge spectra for $\text{La}_{0.7}\text{Ca}_{0.3}\text{Mn}_{1-x}\text{Sc}_x\text{O}_3$ ($x = 0.0, 0.03, \text{ and } 0.05$) oxides. Fourier transform of EXAFS spectra are shown in the inset.

spheres around the EXAFS (Mn) ions in perovskite ABO_3 cells. Intensity of the OP peak decreases with x increase because the Mn atom content decreases at strontium doping. Also a minor decrease of the AP peak with x is observed. It manifests the decrease of the Mn – Sr, Ca pairs in the perovskites lattice.

To make a nature of the change of properties of the studied *B*-site substituted manganites cleaner the XANES spectra at Mn *L*- and O *K*-edges were measured.

Fig. 4 shows Mn *L*-edge spectra for the LCMnSc perovskites. The spectra are split into $L_3(2p_{3/2})$ and $L_2(2p_{1/2})$ main peaks at 642.0 and 652.4 eV which caused by the core hole spin-orbit coupling. The both peaks are additionally split by crystal field which associated with the orbital t_{2g} and e_g symmetry states. The L_3 spectra show also the fine structure which manifested by the appearance of smoothed shoulders which were also observed at studying the *B*-site substituted [26,27], vacancy-doped [28] manganites, and in-situ catalysis in perovskites [29]. With the x increase the peak positions of the Mn *L*-edge lines (as well as the Mn *K*-edge positions) remain almost constant indicating for the unvaried manganese valence and that the valence is higher than 3+, that indicated by the position of the peaks. The intensity of the Mn *L*-edge peaks decreases essentially. The above decrease could be associated with the decrease of the Mn^{3+} content and, according to DE model [2], causes the T_C decrease. The conclusion is in line with that pronounced at study of self-doped $\text{La}_{1-x}\text{MnO}_{3+\delta}$ manganites [28]. Also, parallel change of L_3 and L_2 peak intensity with the conductivity was observed at studying $\text{La}_{0.5}\text{Sr}_{0.5}(\text{Fe},\text{Ti},\text{Ta})\text{O}_{3-\delta}$ [26], and $\text{La}_{0.5}\text{Sr}_{0.5}\text{Fe}_{0.75}\text{Ni}_{0.25}\text{O}_3$ and $\text{LaFe}_{0.75}\text{Ni}_{0.25}\text{O}_3$ [27] oxides. Remarkably, essential change of the shape as well as the position of the L_3 peak was observed at studying the in-situ catalysis of

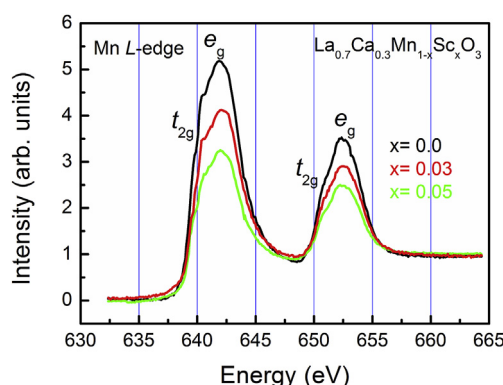


Fig. 4. Mn *L*-edge spectra for $\text{La}_{0.7}\text{Ca}_{0.3}\text{Mn}_{1-x}\text{Sc}_x\text{O}_3$ ($x = 0.0, 0.03, \text{ and } 0.05$) oxides.

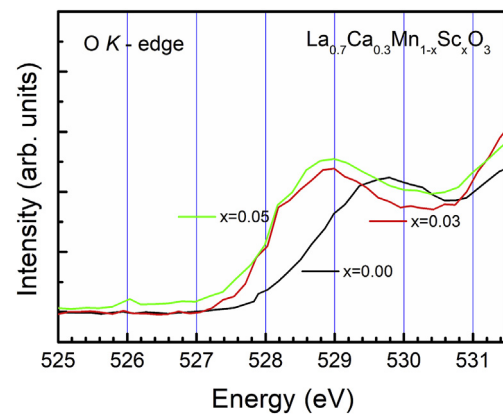


Fig. 5. Oxygen *K*-edge spectra for $\text{La}_{0.7}\text{Ca}_{0.3}\text{Mn}_{1-x}\text{Sc}_x\text{O}_3$ ($x = 0.0, 0.03, \text{ and } 0.05$) perovskites.

$\text{Pr}_{1-x}\text{Ca}_x\text{MnO}_3$ perovskites, the change was also manifested as the decrease of the L_3 - L_2 separation and attributed to an intermediate $\text{Mn}^{3+/\text{4}+}$ oxidation state instead of $\text{Mn}^{3+}/\text{Mn}^{4+}$ species [29].

Fig. 5 shows the O *K*-edge spectra of the sintered perovskites. The spectra show the pre-peak with maxima at 529–530 eV, beginning of low-energy edge tail of the spectra determines the Fermi level of manganites [30]. Pre-edge is associated with the hybridization between the Mn *3d* and O *2p* states and indicates for the hole nature of the LCMnSc oxides introduced by the divalent (calcium) doping [31,32]. The pre-peak position shifts to low energy with x increase. The shift of the O *K* – pre-edge is very similar to that observed by Toulemonde et al. in the study of $\text{PrMn}^{3+}\text{O}_3$, $\text{Pr}_{0.7}\text{Ca}_{0.15}\text{Sr}_{0.15}\text{Mn}^{3+/4+}\text{O}_3$ and $\text{CaMn}^{4+}\text{O}_3$ oxides [31]. Namely, for the studied $\text{La}_{0.7}\text{Ca}_{0.3}\text{Mn}_{1-x}\text{Sc}_x\text{O}_3$ perovskites the formal manganese valence increases with x and oxygen *K*-pre-edge shifts to low energy. It could be supposed that decrease of the T_C , caused by the x increase, is strongly connected with the change of hybridization of O *2p* and Mn *3d* states which is revealed by the observed shift of the oxygen *K*-pre-peak. Notable, according to the results for *B* [26] – and *A*- [33] site substituted manganites a pre-peak of oxygen *K*-edge spectra correlates with the conductivity, σ .

4. Conclusions

Change of electron hybridization states in $\text{La}_{0.7}\text{Ca}_{0.3}\text{Mn}_{1-x}\text{Sc}_x\text{O}_3$ ($x = 0.0; 0.03, \text{ and } 0.05$) perovskites is revealed. This is manifested by the change of Mn *L*-edge line intensity and shifting of O *K*-edge position which are parallel to observed T_C changes, which, in turn, are parallel to the change of x -value. The result differs from that observed for the hole doped $\text{La}_{1-z}\text{D}_z\text{MnO}_3$ manganites where the change of Curie temperature was consistent with the change of average manganese valence and manifested by the change in position of the Mn *K*-edge. The change of average and local crystal structure caused by the larger Sc^{3+} than the Mn^{3+} ions are observed with the x-ray diffraction and Fourier transform of the EXAFS spectra.

Acknowledgements

The reported study was funded by Russian Foundation for Basic Research according to the project No. 18-08-01071 A. The authors are also indebted to N.Yu. Starostyuk for the help at preparing the samples.

References

- [1] J.M.D. Coey, M. Viret, S. Von Molnár, Mixed-valence manganites, *Adv. Phys.* 58 (2009) 571–697.
- [2] C. Zener, Interaction between the *d*-shells in the transition metals. II. Ferromagnetic compounds of manganese with perovskite structure, *Phys. Rev.* 82 (1951) 403–405.
- [3] G. Subías, J. García, M. Proietti, J. Blasco, X-ray-absorption near-edge spectroscopy and circular magnetic x-ray dichroism at the Mn edge of magneto-resistive manganites, *Phys. Rev. B* 56 (1997) 8183–8191.
- [4] A.Y. Ignatov, N. Ali, S. Khalid, Mn *K*-edge XANES study of the $\text{La}_{1-x}\text{Ca}_x\text{MnO}_3$ colossal magnetoresistive manganites, *Phys. Rev. B* 64 (2001), 014413.
- [5] A.N. Ulyanov, J.S. Kim, Y.M. Kang, D.G. Yoo, S.I. Yoo, Oxygen deficiency as a driving force for metamagnetism and large low field magnetocaloric effect in $\text{La}_{0.7}\text{Ca}_{0.3-x}\text{Sr}_x\text{MnO}_{3-\delta}$ manganites, *J. Appl. Phys.* 104 (2008) 113916.
- [6] H. Zhang, Y. Li, H. Liu, X. Dong, K. Chen, Q. Hou, Q. Li, Disappearance of Griffiths phase in polycrystalline sample $\text{La}_{0.75}\text{Ca}_{0.15}\text{MnO}_{3-\delta}$ with controlling oxygen vacancy, *J. Supercond. Nov. Magnetism* 25 (2012) 2365–2370.
- [7] A.N. Ulyanov, N.E. Pismenova, D.S. Yang, V.N. Krivoruchko, G.G. Levchenko, Local structure, magnetization and Griffiths phase of self-doped $\text{La}_{1-x}\text{MnO}_{3+\delta}$ manganites, *J. Alloys Compd.* 550 (2013) 124–128.
- [8] A.N. Ulyanov, S.V. Savilov, A.V. Sidorov, A.V. Vasiliev, N.E. Pismenova, E.A. Goodilin, Electron structure, Raman “vacancy” modes and Griffiths-like phase of self-doped $\text{Pr}_{1-x}\text{MnO}_{3+\delta}$ manganites, *J. Alloys Compd.* 722 (2017) 77–82.
- [9] V. Punith Kumar, R.L. Hadimani, D. Paladhi, T.K. Nath, D.C. Jiles, V. Dayal, Investigation of magnetic interactions, electrical and magneto-transport properties in Ga-substituted $\text{La}_{0.4}\text{Bi}_{0.6}\text{MnO}_3$ perovskite manganites, *Mater. Sci. Eng. B* 209 (2016) 75–86.
- [10] A.N. Ulyanov, S.-C. Yu, Local structure and destruction of electron pathway effects on Curie temperature of *B*-site-substituted lanthanum manganites, *J. Appl. Phys.* 97 (2005) 10H702.
- [11] D.K. Pandey, A. Modi, K. Dubey, P. Pandey, V. Sharma, G.S. Okram, N.K. Gaur, Influence of Al doping on the magnetoresistance and transport properties of $\text{La}_{0.7}\text{Ba}_{0.3}\text{Mn}_{1-x}\text{Al}_x\text{O}_3$ ($0 \leq x \leq 0.15$) manganites, *J. Magn. Magn. Mater.* 471 (2019) 153–163.
- [12] E. Elyana, Z. Mohamed, S.A. Kamil, S.N. Supardan, S.K. Chen, A.K. Yahya, Revival of ferromagnetic behavior in charge-ordered $\text{Pr}_{0.75}\text{Na}_{0.25}\text{MnO}_3$ manganite by ruthenium doping at Mn site and its MR effect, *J. Solid State Chem.* 258 (2018) 191–200.
- [13] A.N. Ulyanov, A.V. Vasiliev, E.A. Eremina, O.A. Shlyakhtin, S.V. Savilov, E.A. Goodilin, Phenomenological description of doped manganites. Electron bandwidth, crystal local structure and Curie temperature, *Ceram. Int.* 44 (2018) 22297–22300.
- [14] Z. Liu, W.G. Lin, K.W. Zhou, J.L. Yan, Effect of Cu doping on the structural, magnetic and magnetocaloric properties of $\text{La}_{0.7}\text{Sr}_{0.25}\text{Na}_{0.05}\text{Mn}_{1-x}\text{Cu}_x\text{O}_3$ manganites, *Ceram. Int.* 44 (2018) 2797–2802.
- [15] A. Dhahri, E. Dhahri, E.K. Hii, Giant magnetoresistance and correlation between critical behavior and electrical properties in a new compound $\text{La}_{0.6}\text{Gd}_{0.1}\text{Sr}_{0.3}\text{Mn}_{0.8}\text{Si}_{0.2}\text{O}_3$ manganite, *J. Alloys Compd.* 727 (2017) 449–459.
- [16] P.J. Lampen, Y. Zhang, T.L. Phan, P. Zhang, S.C. Yu, H. Srikanth, M.H. Phan, Magnetic phase transitions and magnetocaloric effect in $\text{La}_{0.7}\text{Ca}_{0.3}\text{Mn}_{1-x}\text{Fe}_x\text{O}_3$ ($0.00 \leq x \leq 0.07$) manganites, *J. Appl. Phys.* 112 (2012) 113901.
- [17] G.F. Wang, Z.R. Zhao, H.L. Li, X.F. Zhang, Magnetocaloric effect and critical behavior in Fe-doped $\text{La}_{0.67}\text{Sr}_{0.33}\text{Mn}_{1-x}\text{Fe}_x\text{O}_3$ manganites, *Ceram. Int.* 42 (2016) 18196–18203.
- [18] W. Ncib, A. Ben Jazia Kharrat, M.A. Wederni, N. Chniba-Boudjada, K. Khirouni, W. Boujelben, Investigation of structural, electrical and dielectric properties of sol-gel prepared $\text{La}_{0.67-x}\text{Eu}_x\text{Ba}_{0.33}\text{Mn}_{0.85}\text{Fe}_{0.15}\text{O}_3$ ($x=0.0, 0.1$) manganites, *J. Alloys Compd.* 768 (2018) 249–262.
- [19] J.M. De Teresa, P.A. Algarabel, C. Ritter, J. Blasco, M.R. Ibarra, L. Morellon, J.I. Espeso, J.C. Gómez-Sal, Possible quantum critical point in $\text{La}_{2/3}\text{Ca}_{1/3}\text{Mn}_{1-x}\text{Ga}_x\text{O}_3$, *Phys. Rev. Lett.* 94 (2005) 207205.
- [20] M. Pekala, J. Mucha, B. Vertruyen, R. Cloots, M. Ausloos, Effect of Ga doping on magneto-transport properties in colossal magnetoresistive $\text{La}_{0.7}\text{Ca}_{0.3}\text{Mn}_{1-x}\text{Ga}_x\text{O}_3$ ($0 < x < 0.1$), *J. Magn. Magn. Mater.* 306 (2006) 181–190.
- [21] R.D. Shannon, Revised effective ionic radii and systematic studies of interatomic distances in halides and chalcogenides, *Acta Crystallogr. A* 32 (1976) 751–767.
- [22] Y.H. Huang, C.S. Liao, Z.M. Wang, X.H. Li, C.H. Yan, J.R. Sun, B.G. Shen, Large lattice effects arising from Sc on magnetic and transport properties in $\text{La}_{0.7}\text{Ca}_{0.3}\text{Mn}_{1-x}\text{Sc}_x\text{O}_3$, *Phys. Rev. B* 65 (2002) 184423.
- [23] A.N. Ulyanov, S.-C. Yu, D.-S. Yang, Mn-site-substituted lanthanum manganites: destruction of electron pathway and local structure effects on Curie temperature, *J. Magn. Magn. Mater.* 282 (2004) 303–306.
- [24] G. Dezanneau, M. Audier, H. Vincent, C. Meneghini, E. Djurado, Structural characterization of $\text{La}_{1-x}\text{MnO}_{3+\delta}$ by x-ray diffraction and x-ray absorption spectroscopy, *Phys. Rev. B* 69 (2004), 014412.
- [25] B. Zhang, C.J. Sun, J.S. Chen, T. Venkatesan, S.M. Heald, G. Moog Chow, Temperature dependent electronic structure of $\text{Pr}_{0.67}\text{Sr}_{0.33}\text{MnO}_3$ film probed by X-ray absorption near edge structure, *J. Appl. Phys.* 115 (2014) 17E116.
- [26] A. Braun, D. Bayraktar, S. Erat, A.S. Harvey, D. Beckel, J.A. Purton, P. Holtappels, L.J. Gauckler, T. Graule, Pre-edges in oxygen (1s) x-ray absorption spectra: a spectral indicator for electron hole depletion and transport blocking in iron perovskites, *Appl. Phys. Lett.* 94 (2009) 202102.
- [27] S. Erat, H. Wadati, F. Aksoy, Z. Liu, T. Graule, L.J. Gauckler, A. Braun, Iron-resonant valence band photoemission and oxygen near edge x-ray absorption fine structure study on $\text{La}_{1-x}\text{Sr}_x\text{Fe}_{0.75}\text{Ni}_{0.25}\text{O}_{3-\delta}$, *Appl. Phys. Lett.* 97 (2010) 124101.
- [28] A.N. Ulyanov, H.J. Shin, D.S. Yang, S.V. Savilov, N.E. Pismenova, E.A. Goodilin, Hybridization of electronic states and magnetic properties of self-doped $\text{La}_{1-x}\text{MnO}_{3+\delta}$ ($0 \leq x \leq 0.15$) perovskites: XANES study, *J. Magn. Magn. Mater.* 458 (2018) 134–136.
- [29] D. Mierwaldt, S. Mildner, R. Arrigo, A. Knop-Gericke, E. Franke, A. Blumenstein, J. Hoffmann, C. Jooss, In situ XANES/XPS investigation of doped manganese perovskite catalysts, *Catalysts* 4 (2014) 129–145.
- [30] D.D. Sarma, O. Rader, T. Kachel, A. Chainani, M. Mathew, K. Hollidak, W. Gudat, W. Eberhardt, Contrasting behavior of homovalent-substituted and hole-doped systems: O K-edge spectra from $\text{LaNi}_{1-x}\text{M}_x\text{O}_3$ ($\text{M}=\text{Mn}, \text{Fe}$, and Co) and $\text{La}_{1-x}\text{Sr}_x\text{MnO}_3$, *Phys. Rev. B* 49 (1994) 14238–14243.
- [31] O. Toulemonde, F. Millange, F. Studer, B. Raveau, J.H. Park, C.T. Chen, Changes in the Jahn-Teller distortion at the metal-insulator transition in CMR manganites ($\text{Pr}, \text{Nd}_{0.7}(\text{Sr}, \text{Ca})_{0.3}\text{MnO}_3$), *J. Phys. Condens. Matter* 11 (1999) 109–120.
- [32] N. Mannella, C.H. Booth, A. Rosenhahn, B.C. Sell, A. Nambu, S. Marchesini, B.S. Mun, S.H. Yang, M. Watanabe, K. Ibrahim, E. Arenholz, A. Young, J. Guo, Y. Tomioka, C.S. Fadley, Temperature-dependent evolution of the electronic and local atomic structure in the cubic colossal magnetoresistive manganite $\text{La}_{1-x}\text{Sr}_x\text{MnO}_3$, *Phys. Rev. B* 77 (2008) 125134.
- [33] H. Ju, H.-C. Sohn, K. Krishnan, Evidence for $\text{O}2p$ hole-driven conductivity in $\text{La}_{1-x}\text{Sr}_x\text{MnO}_3$ ($0 \leq x \leq 0.7$) and $\text{La}_{0.7}\text{Sr}_{0.3}\text{MnO}_2$ thin films, *Phys. Rev. Lett.* 79 (1997) 3230–3233.